AIP | Physics of Plasmas
#1 JOURNAL IN 2014 GOOGLE SCHOLAR METRICS FOR THE PLASMA & FUSION CATEGORY

Ion temperature gradient driven turbulence with strong trapped ion resonance

Y. Kosuga, S.-I. Itoh, P. H. Diamond, K. Itoh, and M. Lesur

Citation: Physics of Plasmas **21**, 102303 (2014); doi: 10.1063/1.4897179
View online: http://dx.doi.org/10.1063/1.4897179
View Table of Contents: http://scitation.aip.org/content/aip/journal/pop/21/10?ver=pdfcov
Published by the AIP Publishing

Articles you may be interested in

Shear flow instabilities induced by trapped ion modes in collisionless temperature gradient turbulence
Phys. Plasmas **22**, 042304 (2015); 10.1063/1.4916770

Plasma size and power scaling of ion temperature gradient driven turbulence
Phys. Plasmas **21**, 020706 (2014); 10.1063/1.4867379

Impurity transport driven by ion temperature gradient turbulence in tokamak plasmas
Phys. Plasmas **17**, 062501 (2010); 10.1063/1.3430639

Gyrokinetic secondary instability theory for electron and ion temperature gradient driven turbulence
Phys. Plasmas **14**, 112308 (2007); 10.1063/1.2812703

Kinetic simulation of a quasisteady state in collisionless ion temperature gradient driven turbulence
Phys. Plasmas **9**, 3659 (2002); 10.1063/1.1501823

This article is copyrighted as indicated in the article. Reuse of AIP content is subject to the terms at: http://scitation.aip.org/termsconditions. Downloaded to IP: 35.8.11.3 On: Tue, 26 Jan 2016 19:00:16

Ion temperature gradient driven turbulence with strong trapped ion resonance

Y. Kosuga,[1,2,a)] S.-I. Itoh,[3,2] P. H. Diamond,[4,5] K. Itoh,[6,3] and M. Lesur[2]
[1]*Institute for Advanced Study, Kyushu University, Fukuoka, Japan*
[2]*Research Institute for Applied Mechanics, Kyushu University, Fukuoka, Japan*
[3]*Research Center for Plasma Turbulence, Kyushu University, Fukuoka, Japan*
[4]*CASS and CMTFO, University of California at San Diego, La Jolla, California 92093, USA*
[5]*WCI Center for Fusion Theory, National Fusion Research Institute, Daejeon, South Korea*
[6]*National Institute for Fusion Science, Gifu, Japan*

(Received 21 May 2014; accepted 17 September 2014; published online 7 October 2014)

A theory to describe basic characterization of ion temperature gradient driven turbulence with strong trapped ion resonance is presented. The role of trapped ion granulations, clusters of trapped ions correlated by precession resonance, is the focus. Microscopically, the presence of trapped ion granulations leads to a sharp (logarithmic) divergence of two point phase space density correlation at small scales. Macroscopically, trapped ion granulations excite potential fluctuations that do not satisfy dispersion relation and so broaden frequency spectrum. The line width from emission due only to trapped ion granulations is calculated. The result shows that the line width depends on ion free energy and electron dissipation, which implies that non-adiabatic electrons are essential to recover non-trivial dynamics of trapped ion granulations. Relevant testable predictions are summarized. © *2014 AIP Publishing LLC*. [http://dx.doi.org/10.1063/1.4897179]

I. INTRODUCTION

As plasmas of interest—astrophysical, space, and laboratory (in particular fusion) plasmas—are often collisionless, resonance between waves and particles plays a key role in understanding dynamics of turbulent plasmas. Indeed, resonance between waves and particles is the classic problem in plasma physics, and considerable works have been performed and are still on-going. At the simplest level, resonance can trigger instabilities, such as the bump-on-tail instability and current driven ion acoustic waves. At the nonlinear stage, as turbulent amplitude increases, an increasing number of resonant particles are trapped in waves. In this case, the system shows rich nonlinear behavior, such as the formation of BGK vortices,[1] phase space density holes,[2–6] pairs of clumps and holes,[7–13] and phase space density granulations.[14–17] More recently, state-of-the-art numerical scheme and computational power were applied to study simplified models, such as bump-on-tail[18] and ion-acoustic turbulence.[19] The numerical studies have unambiguously identified that in addition to waves, phase space structures that arise from the electrostatic trapping of particles lead to nonlinear instability, convective transport, and anomalous resistivity.

Resonance between waves and particles is important for fusion plasmas as well. In tokamak plasmas, particles trapped in magnetic mirrors, or "bananas," precess in toroidal direction and can resonate with waves.[20] Since the toroidal precession is essentially 1D motion, we expect that resonance can be strong enough to produce correlated resonating trapped particles, called granulations.[21,22] For example, in trapped ion turbulence,[20,23,24] granulations are predicted to form due to trapped ion precession resonance.[22] Once formed, trapped ion granulations behave as macroparticles and transport ion free energy via dynamical friction with electrons (Fig. 1). The flux is much similar to that in Fokker-Planck theory[15,17,22,25] and is in marked contrast to the conventional quasilinear picture that models transport flux via a diffusive flux. More recently, theory was extended to include coupling between trapped ion granulations and shear flows.[26–28] While so far studies on trapped ion granulations are theoretically oriented, recent developments in computational study allow direct numerical simulation of kinetic models for trapped ion turbulence,[29–31] and a verification study is about to begin. However, before starting detailed comparisons, it is useful and necessary to obtain a basic characterization of turbulence with trapped ion granulations. For example, former theory does not treat trapped ion

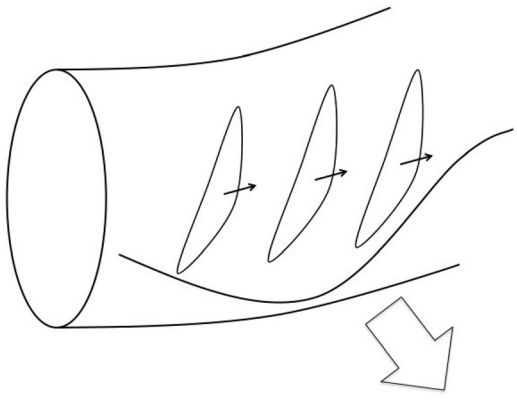

FIG. 1. Schematic view of trapped ion granulations and transport driven by them. Precessing trapped ions resonate with waves and can form a group of correlated resonant bananas. The "bunch of bananas" is dragged from outgoing electrons and leads to release of free energy in ions.

[a)]Electronic mail: kosuga@riam.kyushu-u.ac.jp

 © 2014 AIP Publishing LLC

This article is copyrighted as indicated in the article. Reuse of AIP content is subject to the terms at: http://scitation.aip.org/termsconditions. Downloaded to IP: 35.8.11.3 On: Tue, 26 Jan 2016 19:00:16

granulation correlation function at steady state or estimate the line width of the frequency spectrum. These are typical effects that granulations give rise to[16,21] and can be easily tested.

In this paper, we present a theory to describe basic characteristics of trapped ion granulations, such as basic scales, sharp correlation of phase space density fluctuation at small scales, and broadening of the linewidth (see Fig. 2 for flowchart). At a microscopic level, trapped ion granulations are characterized by the two point phase space density correlation, which is referred to as "phasestrophy."[32] The evolution equation for phasestrophy is derived. Phasestrophy evolution is determined by (i) the production of turbulent fluctuation correlation by dynamical friction and (ii) nonlinear dispersion due to $E \times B$ scattering and difference in toroidal precession speed (Fig. 6). The balance between the two processes leads to a steady state. At the stationary state, the phasestrophy of trapped ions increases logarithmically as the two points in phase space approach. This increase cannot be reproduced from quasilinear estimate, as the quasilinear theory predicts $\langle \delta f(1)\delta f(2)\rangle \propto \tau_c D\langle f\rangle'^2$, which is finite as $1 \to 2$. Here, D is the diffusion coefficient of phase space turbulent flux. Thus, the deviation of phasestrophy from quasilinear level is an indication of the formation of trapped ion granulations. Note that this feature can be tested in numerical experiments. We then derive macroscopic implication by taking energy moment. At the macroscopic level, the stationary state is schematically described in Fig. 7. In this state, granulations extract free energy via dynamical friction and emit waves via Cerenkov emission, which are in turn absorbed in the plasma by the total dissipation. In this state, the fluctuation spectrum contains emissions from granulations, in addition to normal modes. Hence, granulations tend to broaden the spectrum. The degree of spectrum broadening is estimated from the spectrum balance equation.

The remaining of the paper is organized as follows. In Sec. II, we formulate the dynamics of trapped ion granulations by calculating the evolution of the two point phase space density correlation. In Sec. III, the spectrum balance equation is derived by integrating the two point phase space density correlation over energy. We discuss the form of the frequency spectrum in the presence of trapped ion granulations. Section IV contains conclusion and discussion. Testable predictions are summarized in Table I.

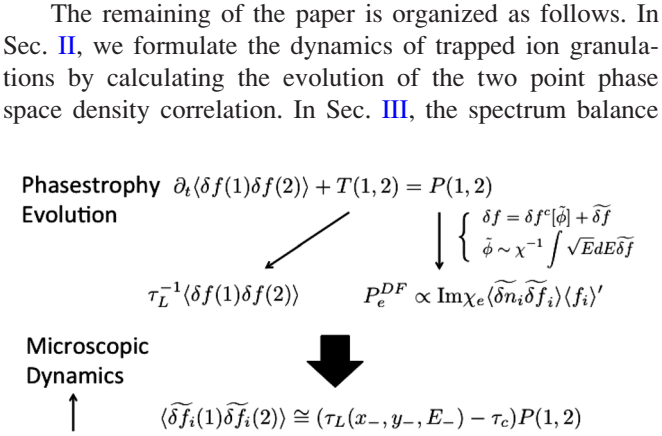

FIG. 2. A flowchart for the structure of the paper. At the microscopic level, the dynamics of trapped ion granulations are formulated by the evolution of two point phase space density correlation. The energy integral yields macroscopic implications, such as spectrum balance equation and frequency line width.

II. EVOLUTION OF TWO POINT PHASE SPACE DENSITY CORRELATION

The dynamics of trapped ion turbulence are described by a simplified model (bounce kinetic equation) by exploiting the difference in time scales.[29–31] As the frequency range of interest is $\omega_{ci}, \omega_{ti}, \omega_{bi} \gg \omega \sim \omega_{Di}$ (ω_{ci} is the ion cyclotron frequency, ω_{ti} is the transit frequency of passing ions, ω_{bi} is the bounce frequency of ions trapped in magnetic mirror, ω is the frequency of interest, and ω_{Di} is the precession frequency), the fast gyro and bounce motions are averaged out. This yields the bounce averaged kinetic equation for trapped ions

$$\partial_t f_i + v_{Di}\bar{E}\partial_x f_i + \frac{c}{B}\hat{z} \times \nabla\phi \cdot \nabla f_i = 0. \tag{1}$$

Here, $\bar{E} \equiv E/T_i$ is the normalized energy. The equation is arguably the simplest model that captures kinetic effects (resonance dynamics) on the spatial $E \times B$ convection. Note that this follows from the fact that the parallel acceleration term is annihilated by the bounce average. Thus, the energy is not scattered in this model, which allows us to focus on spatial $E \times B$ mixing, *along with the effect of resonance from precession motion*. Electrons are assumed to be dissipative, thus $n_e/n_0 = (1 - i\delta_{col})(e\phi/T_e)$, where δ_{col} is the phase shift due to collisions. The set of equations is made self-consistent via the quasi-neutrality condition

$$n_e = -\frac{e\phi}{T_i} + \sqrt{2\epsilon_0}\frac{2}{\sqrt{\pi}}\left(\frac{2\pi T_i}{m_i}\right)^{3/2}\int \sqrt{\bar{E}}d\bar{E}f_i + \rho^2\nabla_\perp^2\frac{e\phi}{T_e}. \tag{2}$$

Here, the first term in the right hand side is from passing ions, the second term is from trapped ions, and the last term includes polarization charge both from classical and neoclassical effects,[33] $\rho^2 = \rho_s^2(1 + 1.6q^2/\sqrt{\epsilon_0})$.

Although the simplicity of the model is one of the reason why we focus on trapped ion turbulence, we also note that trapped ion turbulence can be important for transport dynamics in toroidal plasmas. This is since *trapped ion turbulence can drive transport which is unique compared to that driven by other micro-turbulence*. Since trapped ion mode is characterized by long wave length and long coherence time,[20] it is quite likely that structures, such as convective cells[24] or granulations,[16,22] may form in trapped ion turbulence. For example, once formed, granulations drive transport, which is not determined by conventional quasilinear flux, but by Lenard-Balescu flux with dynamical friction.[22,25] Thus, transport by trapped ion turbulence has quite different character from that driven by other micro-turbulence. We also note that zonal flows are also important in trapped ion turbulence dynamics with granulations, since trapped ion

This article is copyrighted as indicated in the article. Reuse of AIP content is subject to the terms at: http://scitation.aip.org/termsconditions. Downloaded to IP: 35.8.11.3 On: Tue, 26 Jan 2016 19:00:16

granulations may scatter polarization charge and generate zonal flows.[27]

In order to elaborate the unique feature of trapped ion turbulence, here we compare typical time scales of interest, the auto-correlation time of spectra $\tau_{ac} \sim |d\omega_{\mathbf{k}}/dk_\theta - \omega_{\mathbf{k}}/k_\theta|^{-1}\Delta k_\theta^{-1}$, and the "circulation" time of resonating trapped ions $\tau_{circ} \sim (\omega_{di}\Delta E)^{-1}$. Here, Δk_θ is the width of wave number spectra, $\Delta E \sim 1/(\tau_c\omega_{di})$ is the resonance width, and τ_c is the turbulence correlation time. Note that $\tau_{circ} \sim \tau_c$, thus the circulation time of resonating particles is given by $E \times B$ circulation time. In trapped ion turbulence, the condition $\tau_{ac} \gtrsim \tau_{circ}$ is easily satisfied, since modes are peaked at long wave length ($\omega_{\mathbf{k}} < \omega_{bi} \Longleftrightarrow k_\theta\rho_i < \epsilon_0/q$) and thus $\tau_{ac} = ((1+k_\perp^2\rho^2)^2/2k_\theta^2\rho^2)(k_\theta/\Delta k_\theta)(\sqrt{2\epsilon_0}\omega_*)^{-1}$ can be long, even for broad spectra $\Delta k_\theta/k_\theta \sim O(1)$. In this case, the cluster of resonant particles within the energy width $\Delta E \sim 1/(\tau_c\omega_{di})$, called trapped ion granulations, causes irreversible mixing and determines turbulence dynamics. We are interested in this situation and shall discuss how trapped ion granulations impact turbulence dynamics in the following. See Fig. 3 for parameter regime of interest.

Turbulence resonance dynamics for $K \gtrsim O(1)$ are illustrated by considering wave packet dynamics for different Kubo numbers. Here, we use a model spectrum

$$\phi(\mathbf{x},\mathbf{y},t) = \mathrm{Re}\sum_{\mathbf{k}} \phi_{\mathbf{k}} e^{ik_x x + ik_y y - i\omega_{\mathbf{k}}t}, \tag{3}$$

$$\phi_{\mathbf{k}} = \phi_0 \exp\left[-\frac{(k_x-k_{x0})^2}{2\Delta k_x^2} - \frac{(k_y-k_{y0})^2}{2\Delta k_y^2}\right]. \tag{4}$$

Using the dispersion relation for trapped ion modes, expanding the phase around (k_{x0}, k_{y0}) and integrating over $\mathbf{k}$ yield

$$\hat{\phi} = -\cos(k_{x0}x + k_{y0}y - \omega_{\mathbf{k_0}}t)\exp\left[-\frac{\Delta k_x^2}{2}\left(x - \frac{\partial\omega_{\mathbf{k}_0}}{\partial k_{x0}}t\right)^2 - \frac{\Delta k_y^2}{2}\left(y - \frac{\partial\omega_{\mathbf{k}_0}}{\partial k_{y0}}t\right)^2\right]. \tag{5}$$

Here, the potential is normalized to be -1 at $t=0$ and $(x, y) = (0, 0)$. Noting that $k_{x0}k_{y0} < 0$ for $\partial\omega_{\mathbf{k}_0}/\partial k_{x0} > 0$ and assuming for simplicity that $|k_{x0}| \sim |k_{y0}| \sim k_0$, $\Delta k_x \sim \Delta k_y \sim k_0$ and $|\omega_{\mathbf{k}_0}| \sim \tau_{circ}^{-1}$, we have

$$\hat{\phi} = -\cos\left(-k_0x + k_0y + \frac{t}{\tau_{circ}}\right)\exp\left[-\frac{1}{2}\left(k_0x - \frac{1}{K}\frac{t}{\tau_{circ}}\right)^2 - \frac{1}{2}\left(k_0y + \frac{t}{\tau_{circ}} + \frac{1}{K}\frac{t}{\tau_{circ}}\right)^2\right]. \tag{6}$$

Here, $K = ((1+k_{\perp 0}^2\rho^2)^2/2k_{y0}^2\rho^2)(k_{y0}/\Delta k_y)(\sqrt{2\epsilon_0}\omega_*\tau_{circ})^{-1}$ is the Kubo number. $\hat{\phi}$ is plotted in Figs. 4 and 5. In the both figures, x and y are normalized by k_0 and t is normalized by τ_{circ}. Fig. 4 is the initial pattern of the wave packet and Fig. 5 depicts dynamics of the wave packet and unperturbed orbit of a resonant particle for different Kubo numbers. For $K = 0.4$, the wave packet and the resonant particle decorrelate. On the other hand, for $K = 4$, the wave packet is rather coherent and the resonance persists. In this case, it is quite likely that initially resonating particles are correlated and their trajectory starts deforming and producing $E \times B$ Eddy's.

Here, as a caveat, we note that in addition to the precession resonance, the bounce resonance $\omega \sim \omega_{bi}$ may be important.[34–36] When the bounce resonance occurs, the resonance would possibly scatter weakly trapped particles and slow them down. Then, the bounce resonance would produce more deeply trapped particles, which can lead to the formation of granulations.

The dynamics of trapped ion turbulence with granulations are described by two point phase space density correlation,[16,22] or phasestrophy[32]

$$\partial_t\langle\delta f(1)\delta f(2)\rangle + T(1,2) = P(1,2). \tag{7}$$

Here, 1 and 2 denotes two different points in phase space, (x_1, y_1, E_1) and (x_2, y_2, E_2). $\langle\ldots\rangle$ denotes an ensemble average, which is technically evaluated by the average over the center of mass spatial coordinate, $\mathbf{x}_+ \equiv (\mathbf{x}_1 + \mathbf{x}_2)/2$. $T(1, 2)$ and $P(1, 2)$ are given by

$$T(1,2) = v_{Di}\bar{E}_1\frac{\partial}{\partial y_1}\langle\delta f(1)\delta f(2)\rangle + \langle\delta f(2)\tilde{\mathbf{v}}_{E\times B}(1)\cdot\nabla_1\delta f(1)\rangle + (1\leftrightarrow 2), \tag{8}$$

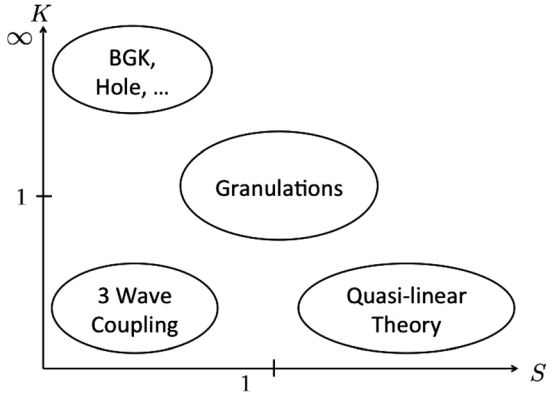

FIG. 3. A schematic view for parameter space of interest.[32] Here, $K \equiv \tau_{ac}/\tau_{circ}$ is the Kubo number and $S \equiv \Delta E/|E_{res}^{n+1} - E_{res}^n|$ is the Chirikov parameter. E_{res}^n is the n-th resonance. We are interested in $K \gtrsim 1$ and $S \gtrsim 1$.

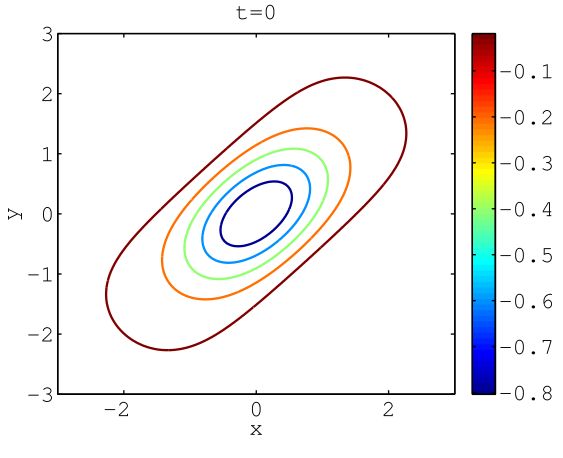

FIG. 4. Initial potential contour produced by Eq. (6).

This article is copyrighted as indicated in the article. Reuse of AIP content is subject to the terms at: http://scitation.aip.org/termsconditions. Downloaded to IP: 35.8.11.3 On: Tue, 26 Jan 2016 19:00:16

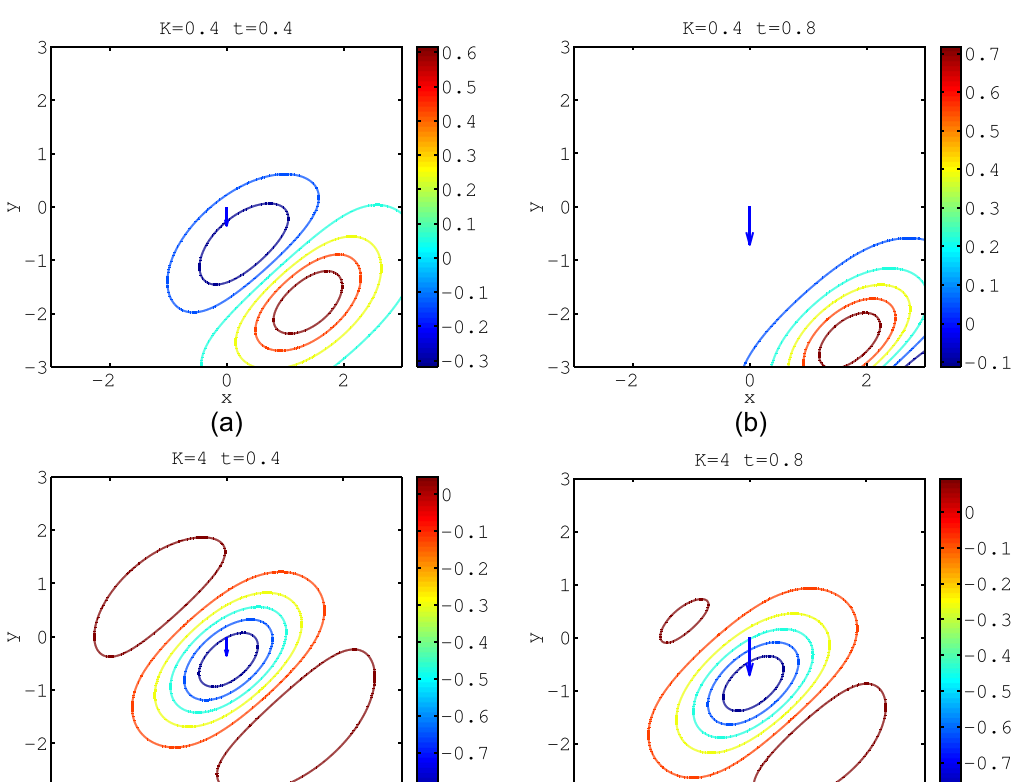

FIG. 5. Dynamics of the wave packet (Eq. (6)) and resonant particles. The arrows indicate unperturbed trajectory of the resonant particles, initially located at (0, 0). For $K = 0.4$, the wave packet and the resonant particle decorrelate. For $K = 4$, the wave packet and the resonant particle maintain resonance. In this case, the formation of trapped ion granulations is quite likely.

$$P(1,2) = -\langle \tilde{v}_{E\times B,x}(1)\delta f(2)\rangle \langle f_i(1)\rangle' + (1 \leftrightarrow 2), \quad (9)$$

where $(1 \leftrightarrow 2)$ denotes the term with the argument exchanged. $T(1, 2)$ describes the decorrelation process due to the difference in the precession speeds and nonlinear $E \times B$ mixing. $P(1, 2)$ is the production term for turbulent fluctuation. Specific forms for $T(1, 2)$ and $P(1, 2)$ are calculated in the following. We note that a similar analysis was performed before, using ballooning formalism.[22] In contrast, here we simply Fourier analyze in (x, y).

A. Closure of the triplet term and extraction of the lifetime of the correlation

$T(1, 2)$ describes mixing process by turbulent $E \times B$ scattering and precession at different speeds (Fig. 6). $T(1, 2)$ requires closure calculation for the triplet nonlinearity. The closure calculation[16,32] can be implemented by calculating phase coherent response of the two point correlation function to $E \times B$ velocity, i.e.,

$$\delta f(2)\tilde{\mathbf{v}}_{E\times B}(1)\cdot\nabla_1\delta f(1) \cong \nabla_1\cdot(\tilde{\mathbf{v}}(1)(\delta f_i(1)\delta f_i(2))^c), \quad (10)$$

where $(\delta f_i(1)\ \delta f_i(2))^c$ in Fourier component is given by

$$(\delta f_i(1)\delta f_i(2))^c_{\mathbf{k}\omega} = -R(1)\tilde{\mathbf{v}}_{\mathbf{k}\omega}e^{i\mathbf{k}\cdot\mathbf{x}_1}\cdot\nabla_1\langle\delta f_i(1)\delta f_i(2)\rangle - R(2)\tilde{\mathbf{v}}_{\mathbf{k}\omega}e^{i\mathbf{k}\cdot\mathbf{x}_2}\cdot\nabla_2\langle\delta f_i(1)\delta f_i(2)\rangle. \quad (11)$$

Here, $R(1,2) = i/(\omega - \omega_{Di}\bar{E}_{1,2} + i/\tau_c)$ is the propagator and τ_c is the turbulence correlation time. Then, the triplet term reduces to

$$\langle\tilde{v}_{E\times B}(1)\delta f(1)\delta f(2)\rangle \cong -\mathbf{D}_{11}\cdot\nabla_1\langle\delta f(1)\delta f(2)\rangle - \mathbf{D}_{12}\cdot\nabla_2\langle\delta f(1)\delta f(2)\rangle. \quad (12)$$

Here, $\mathbf{D}_{11} = \sum_{\mathbf{k}\omega}R(1)\langle\tilde{\mathbf{v}}_{E\times B}\tilde{\mathbf{v}}_{E\times B}\rangle_{\mathbf{k}\omega}$ and $\mathbf{D}_{12} = \sum_{\mathbf{k}\omega}R(2)\langle\tilde{\mathbf{v}}_{E\times B}\tilde{\mathbf{v}}_{E\times B}\rangle_{\mathbf{k}\omega}e^{-i\mathbf{k}\cdot(\mathbf{x}_1-\mathbf{x}_2)}$. Writing in terms of the relative coordinate, $\mathbf{x}_- = \mathbf{x}_1 - \mathbf{x}_2$ and $E_- = E_1 - E_2$, the total mixing term is given by

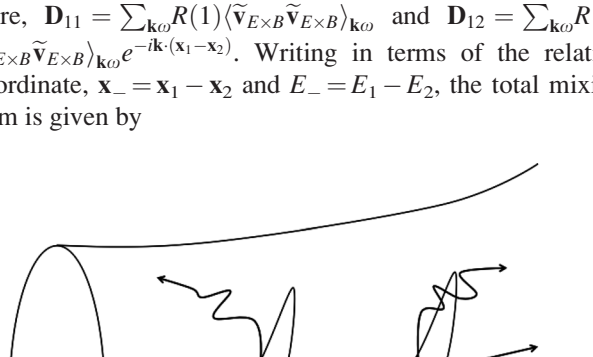

FIG. 6. A cartoon for decorrelation process.[28] Two correlated bananas are decorrelated by (i) turbulent $E \times B$ diffusion and (ii) precession motion at different speeds. The synergy of the processes determines effective lifetime of the correlation.

This article is copyrighted as indicated in the article. Reuse of AIP content is subject to the terms at: http://scitation.aip.org/termsconditions. Downloaded to IP: 35.8.11.3 On: Tue, 26 Jan 2016 19:00:16

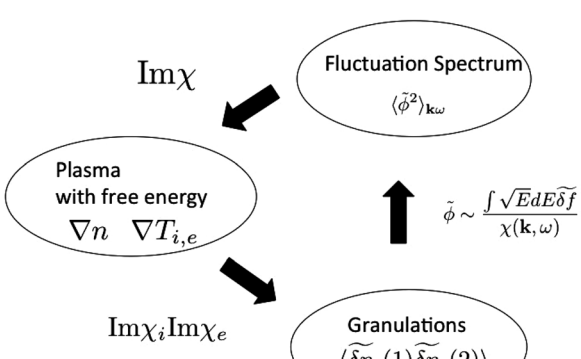

FIG. 7. A schematic view of the balanced state. Trapped ion granulations access free energy via dynamical friction on electrons. Granulations produce "attached" wakes, via Cerenkov emission, which do not satisfy the dispersion relation. Waves in turn are absorbed in plasmas via total dissipation $\propto$ Imχ. The balance among these processes leads to a steady state, which is described by Eq. (37).

$$T(1,2) = v_{Di}\bar{E}_- \frac{\partial}{\partial y_-}\langle \delta f(1)\delta f(2)\rangle - \nabla_- \cdot \mathbf{D}_- \cdot \nabla_- \langle \delta f(1)\delta f(2)\rangle. \quad (13)$$

Here, $\mathbf{D}_- \equiv \mathbf{D}_{11} + \mathbf{D}_{22} - \mathbf{D}_{12} - \mathbf{D}_{21}$ is the strength of the relative dispersion. Note that for large separation, $\mathbf{D}_-$ asymptotes to $2\mathbf{D}_\perp$, where $\mathbf{D}_\perp = \mathbf{D}_{11} = \mathbf{D}_{22}$ is the usual perpendicular diffusion coefficient by turbulent $E\times B$ advection. On the other hand, at small separation $\mathbf{D}_- \cong (\mathbf{k}_0\cdot\mathbf{x}_-)^2\mathbf{D}_\perp$, where $(\mathbf{k}_0\cdot\mathbf{x}_-)^2 \equiv |\sum_{\mathbf{k}\omega}(\mathbf{k}\cdot\mathbf{x}_-)^2 R\langle \tilde{\mathbf{v}}_{E\times B}\tilde{\mathbf{v}}_{E\times B}\rangle_{\mathbf{k}\omega}|/|\sum_{\mathbf{k}\omega} R\langle \tilde{\mathbf{v}}_{E\times B}\tilde{\mathbf{v}}_{E\times B}\rangle_{\mathbf{k}\omega}|$ is the spectral averaged mean wave number. Then, the relative dispersion accelerates as the distance between two points increases. We are interested in the latter regime, as we are interested in the dynamics of correlated resonant particles, which are confined within the typical scales of waves, i.e., $\mathbf{k}_0\cdot\mathbf{x}_- < 1$. Finally, we assume, for simplicity, that the underlying turbulence is isotropic $k_{x,0}\sim k_{y,0}\sim k_0$ and that cross diffusion is small. Then, the total mixing term becomes

$$T(1,2) = v_{Di}\bar{E}_- \frac{\partial}{\partial y_-}\langle \delta f(1)\delta f(2)\rangle - \left(\frac{\partial}{\partial x_-}k_0^2 D_\perp\left(x_-^2+y_-^2\right)\frac{\partial}{\partial x_-} + \frac{\partial}{\partial y_-}k_0^2 D_\perp\left(x_-^2+y_-^2\right)\frac{\partial}{\partial y_-}\right)\langle \delta f(1)\delta f(2)\rangle. \quad (14)$$

Thus, relative dispersion is now determined by the nonlinear $E\times B$ diffusion and precession at different speeds.

The lifetime of correlation is extracted by exploiting the evolution of statistical moments as follows. Here, the statistical moments are defined as $\langle\langle\ldots\rangle\rangle \equiv \int dx_- dy_- dE_-(\ldots)F/\int dx_- dy_- dE_- F$, where $F(t, x_-, y_-, E_-)$ is a probability density function for relative separation and evolves as

$$\partial_t F + v_{Di}\bar{E}_-\frac{\partial}{\partial y_-}F - \left(\frac{\partial}{\partial x_-}k_0^2 D_\perp\left(x_-^2+y_-^2\right)\frac{\partial}{\partial x_-} + \frac{\partial}{\partial y_-}k_0^2 D_\perp\left(x_-^2+y_-^2\right)\frac{\partial}{\partial y_-}\right)F = 0. \quad (15)$$

Evolution of relevant moments is

$$\partial_t\langle\langle x_-^2\rangle\rangle = 6k_0^2 D_\perp\langle\langle x_-^2\rangle\rangle + 2D_\perp k_0^2\langle\langle y_-^2\rangle\rangle, \quad (16)$$

$$\partial_t\langle\langle y_-^2\rangle\rangle = 2v_{Di}\langle\langle \bar{E}_- y_-\rangle\rangle + 2k_0^2 D_\perp\langle\langle x_-^2\rangle\rangle + 6D_\perp k_0^2\langle\langle y_-^2\rangle\rangle, \quad (17)$$

$$\partial_t\langle\langle \bar{E}_- y_-\rangle\rangle = v_{Di}\langle\langle \bar{E}_-^2\rangle\rangle + 2D_\perp k_0^2\langle\langle \bar{E}_- y_-\rangle\rangle, \quad (18)$$

$$\partial_t\langle\langle \bar{E}_-^2\rangle\rangle = 0. \quad (19)$$

The set of equations is solved for initial separation x_-, y_-, E_-. The time asymptotic solution is given by

$$\langle\langle x_-^2\rangle\rangle + \langle\langle y_-^2\rangle\rangle \cong e^{t/\tau_c}\left(x_-^2 + y_-^2 + \frac{8\tau_c v_{Di}\bar{E}_- y_-}{3} + \frac{8\tau_c^2 v_{Di}^2\bar{E}_-^2}{3}\right). \quad (20)$$

Here, $\tau_c \equiv (8k_0^2 D_\perp)^{-1}$. The two points are decorrelated when the relative separation becomes comparable to a typical scale of the field, $\langle\langle x_-^2\rangle\rangle + \langle\langle y_-^2\rangle\rangle \sim k_0^{-2}$. Then, the lifetime of the correlation (a clump of trapped ions) is

$$\tau_{cl} = \tau_c \ln\left[k_0^2 x_-^2 + k_0^2 y_-^2 + \frac{8k_0^2\tau_c v_{Di}\bar{E}_- y_-}{3} + \frac{8\tau_c^2 k_0^2 v_{Di}^2\bar{E}_-^2}{3}\right]^{-1}. \quad (21)$$

Equation (21) is the major product after the closure calculation, $T(1,2) \cong \tau_{cl}^{-1}\langle \delta f(1)\delta f(2)\rangle$. It describes the lifetime of correlated two particles in phase space due to turbulent $E\times B$ mixing and the difference in precession speeds. Note that if ions are cold and do not precess, then the expression reduces to the lifetime due to $E\times B$ mixing only. When ions are hotter and precession becomes important for turbulence dynamics, i.e., $k_0 v_{Di}/\tau_c^{-1} \lesssim 1$, dependence on energy becomes appreciable. We also note that the expression is valid only for the argument of the logarithm is smaller than unity, i.e.,

$$k_0^2 x_-^2 + k_0^2 y_-^2 + \frac{8k_0^2\tau_c v_{Di}\bar{E}_- y_-}{3} + \frac{8\tau_c^2 k_0^2 v_{Di}^2\bar{E}_-^2}{3} < 1. \quad (22)$$

The relation gives the maximum upper bound for the energy difference of two point correlation $\bar{E}_< < \bar{E}_- < \bar{E}_>$, where $\bar{E}_{\{>,<\}} = -y_-/(2\tau_c v_{Di}) \pm (\sqrt{3}\sqrt{1 - k_0^2 x_-^2 - k_0^2 y_-^2/3})/(2\sqrt{2}\tau_c k_0 |v_{di}|))$. The cutoff gives a basic scale in energy space, $\Delta\bar{E} \sim (\tau_c k_0 v_{Di})^{-1}$. Physically, the scale corresponds to the width of the broadened resonance. Particles within ΔE maintain correlation and drive transport.

B. Production term due to granulations

$P(1, 2)$ is the production term for phasestrophy. $P(1, 2)$ with granulations can be calculated by setting $\delta f = \delta f^c + \widetilde{\delta f}$.[16,22,32] Here, δf^c is the coherent response to fluctuating potential and $\delta f^c \propto R\tilde{\phi}$. $\widetilde{\delta f}$ is the incoherent part. Physically, $\widetilde{\delta f}$ arises due to the formation of phase space density granulations. In trapped ion turbulence, $\widetilde{\delta f}$ describes the population of trapped ions correlated by precession resonance. The incoherent part is the analogue of particle discreteness in the test particle model for plasmas close to thermodynamic equilibrium. Following the analogy to the test particle model, we can show that total flux with the

This article is copyrighted as indicated in the article. Reuse of AIP content is subject to the terms at: http://scitation.aip.org/termsconditions. Downloaded to IP: 35.8.11.3 On: Tue, 26 Jan 2016 19:00:16

incoherent contribution is determined, not by quasilinear diffusive flux but by Fokker-Planck flux with dynamical friction[15,25] $\langle \tilde{v}_x \delta f \rangle = -D\langle f \rangle' \rightarrow -D\langle f \rangle' + F\langle f \rangle$. Here, the diffusive flux arises from the coherent response and the dynamical friction is due to the incoherent contribution.

A specific form for production term is calculated for trapped ion turbulence. In order to elucidate the role of granulations in microscopic dynamics, here we assume that eigenmodes are oversaturated and fluctuations are supported from the emission from granulations. In this case, the quasi-neutrality condition gives

$$\frac{e\widetilde{\phi}_{\mathbf{k}\omega}}{T_e} = \frac{1}{\chi(\mathbf{k},\omega)} 8\pi\sqrt{\epsilon_0} v_{thi}^3 \int \sqrt{\bar{E}} d\bar{E} \delta\widetilde{f}_{i,\mathbf{k}\omega} = \frac{1}{\chi(\mathbf{k},\omega)} \frac{\widetilde{\delta n_{i,\mathbf{k}\omega}}}{n_0}. \tag{23}$$

Here, $\chi(\mathbf{k}, \omega)$ is susceptibility. Specific form of $\chi(\mathbf{k}, \omega)$ for linear response is given in the Appendix. Substituting the potential for the production term, we have

$$\begin{aligned} P(1,2) &= \mathrm{Re}\sum_{\mathbf{k}\omega} k_\theta^2 \rho_s^2 c_s^2 R_{\mathbf{k}\omega}(2) \left\langle \left(\frac{e\widetilde{\phi}}{T_e} \right)^2 \right\rangle_{\mathbf{k}\omega} e^{-i\mathbf{k}\cdot\mathbf{x}_-} \langle f_i \rangle'(1) \langle f_i \rangle'(2) \\ &- \sum_{\mathbf{k}\omega} k_\theta \rho_s c_s \frac{\mathrm{Im}\chi_i}{|\chi(\mathbf{k},\omega)|^2} \left\langle \frac{\widetilde{\delta n_i}}{n_0} \delta\widetilde{f}_i(2) \right\rangle_{\mathbf{k}\omega} e^{i\mathbf{k}\cdot\mathbf{x}_-} \langle f_i \rangle'(1) \\ &+ \sum_{\mathbf{k}\omega} k_\theta \rho_s c_s \frac{\mathrm{Im}\chi_e}{|\chi(\mathbf{k},\omega)|^2} \left\langle \frac{\widetilde{\delta n_i}}{n_0} \delta\widetilde{f}_i(2) \right\rangle_{\mathbf{k}\omega} e^{i\mathbf{k}\cdot\mathbf{x}_-} \langle f_i \rangle'(1) \\ &+ (1 \leftrightarrow 2). \end{aligned} \tag{24}$$

The first term is the production due to the diffusive flux, $\propto D_\perp \langle f \rangle'^2$. The second term is from dynamical friction exerted on ions. Note that the first and second terms cancel[22] upon substituting the resonance delta function for propagator $\mathrm{Re}R = \pi\delta(\omega - \omega_{Di}\bar{E})$, the ballistic spectrum $\langle \delta\widetilde{f}_i(1)\delta\widetilde{f}_i(2)\rangle_{\mathbf{k}\omega} \cong \langle \delta\widetilde{f}_i(1)\delta\widetilde{f}_i(2)\rangle_{\mathbf{k}} 2\pi\delta(\omega - \omega_{Di}\bar{E}_+)$, and the linear susceptibility for $\mathrm{Im}\chi_i$. The cancellation is ensured by the 1D resonance structure and we note that any modification to the resonance function, such as the shear flow Doppler resonance, can weaken or eliminate the cancellation.[27] However, for simplicity, we assume that cancellation occurs here. The third term is due to dynamical fiction exerted on electrons (Fig. 1). In this process, the free energy stored in ions is released via trapped ion granulations dragged by electrons. The process arises as a consequence of charge balance constraint on relaxation. Dissipation by electrons is required to trigger the free energy release through this channel. The production term is further simplified by using the pole approximation, $1/|\chi(\mathbf{k},\omega)|^2 \cong 1/((\partial\chi/\partial\omega_{\mathbf{k}})^2(\omega - \omega_{\mathbf{k}})^2 + |\mathrm{Im}\chi|^2)$, where $\omega_{\mathbf{k}}$ is the root of $\mathrm{Re}\chi(\omega, \mathbf{k}) = 0$, and by integrating over ω to obtain

$$P(1,2) \cong \sum_{\mathbf{k}} \frac{k_\theta \rho_s c_s \mathrm{Im}\chi_e}{|\partial\chi/\partial\omega_{\mathbf{k}}||\mathrm{Im}\chi|} \left\langle \frac{\widetilde{\delta n_i}}{n_0} \delta\widetilde{f}_i(2) \right\rangle_{\mathbf{k}} \times \pi\delta(\omega_{\mathbf{k}} - \omega_{Di}\bar{E}_2) e^{i\mathbf{k}\cdot\mathbf{x}_-} \langle f_i \rangle'(1) + (1 \leftrightarrow 2). \tag{25}$$

In the limit $1 \rightarrow 2$, $P(1, 2)$ is finite and is given by

$$\begin{aligned} &\lim_{1\rightarrow 2} P(1,2) \\ &\equiv P(\bar{E}_+) = \sum_{\mathbf{k}} \frac{2\mathrm{Im}\chi_i \mathrm{Im}\chi_e}{|\partial\chi/\partial\omega_{\mathbf{k}}||\mathrm{Im}\chi|} \frac{\delta(\bar{E}_+ - \bar{E}_{\mathbf{k}}^{res})}{8\pi v_{thi}^3 \sqrt{\epsilon_0}\sqrt{\bar{E}_{\mathbf{k}}^{res}}} \\ &\times \left\langle \frac{\widetilde{\delta n_i}}{n_0} \delta\widetilde{f}_i(\bar{E}_{\mathbf{k}}^{res}) \right\rangle_{\mathbf{k}}, \end{aligned} \tag{26}$$

where $\bar{E}_{\mathbf{k}}^{res} \equiv |\omega_{\mathbf{k}}/\omega_{Di}|$ is the resonant energy. Here, linear response for $\mathrm{Im}\chi_i$ was used to write P in compact form. Finally, we note that the production process is tied to release of free energy and describes transport process. The associate transport flux can be extracted from the production term and is given by

$$F = -\sum_{\mathbf{k}} \frac{k_\theta \rho_s c_s \mathrm{Im}\chi_e}{|\partial\chi/\partial\omega_{\mathbf{k}}||\mathrm{Im}\chi|} \left\langle \frac{\widetilde{\delta n_i}}{n_0} \delta\widetilde{f}_i \right\rangle_{\mathbf{k}} \pi\delta(\omega_{\mathbf{k}} - \omega_{Di}\bar{E}_2). \tag{27}$$

Thus, within the approximation used above, transport process by trapped ion granulations is determined by *dynamical friction* on electrons.[22] (See Fig. 1 for schematics.) Electron dissipation is important to access the free energy via dynamical friction, as manifested its dependence via $\mathrm{Im}\chi_e \propto \nu_e^{-1}$.

C. Phase space density correlation at stationary state

Summarizing the results obtained so far, we have phasestrophy evolution as

$$\partial_t \langle \delta f(1)\delta f(2)\rangle + \tau_{cl}^{-1} \langle \delta f(1)\delta f(2)\rangle = P(1,2). \tag{28}$$

τ_{cl}^{-1} is given by Eq. (21) and describes the lifetime of the correlation by mixing due to $E \times B$ scattering and toroidal precession at different speeds. $P(1, 2)$ acts as source for phasestrophy. Specific form for $P(1, 2)$ was given by Eq. (26), which describes source arising from free energy release by trapped ion granulations via dynamical friction on electrons. The two processes balance one another at stationary state. At the stationary state, we have

$$\langle \delta f_i(1)\delta f_i(2)\rangle \cong \tau_{cl}(x_-, y_-, E_-) P(1,2). \tag{29}$$

We note that phasestrophy includes both coherent and incoherent parts. Subtracting $\langle \delta f_i^c \delta f_i^c \rangle$ and $\langle \delta f^c \delta\widetilde{f} \rangle$ from the total phasestrophy gives phasestrophy due to incoherent part. Since[37] $\langle \delta f_i^c \delta f_i^c \rangle = 2\tau_c \mathcal{D}$ and $\langle \delta f^c \delta\widetilde{f} \rangle = \tau_c \mathcal{F}$, where $\mathcal{D}$ is the production due to diffusive flux and $\mathcal{F}$ is the production due to dynamical friction, the correlation of incoherent part is given by

$$\langle \delta\widetilde{f}_i(1)\delta\widetilde{f}_i(2)\rangle \cong (\tau_{cl}(x_-, y_-, E_-) - \tau_c) P(1,2). \tag{30}$$

Equation (30) describes the correlation of two *resonant* particles in two phase space points. Importantly, Eq. (30) implies that at small scales the correlation sharply (logarithmically) increases. This can be seen by taking the limit $1 \rightarrow 2$, where τ_{cl} increases logarithmically while $P(1, 2)$ is finite. The sharp increase should be contrasted to behavior of the correlation for coherent response, $\langle \delta f_i^c \delta f_i^c \rangle = 2\tau_c \mathcal{D} \propto \tau_c D_\perp \langle f \rangle'^2$, which

This article is copyrighted as indicated in the article. Reuse of AIP content is subject to the terms at: http://scitation.aip.org/termsconditions. Downloaded to IP: 35.8.11.3 On: Tue, 26 Jan 2016 19:00:16

is finite as $1 \to 2$. Thus, the presence of granulations increases small scale correlation to the level above that is predicted by quasilinear theory. This feature may be tested in numerical experiment. We note that similar procedure has been implemented before.[38–40] Revisiting similar numerical experiment with continuum code of today merits further study.

Sharp increase of two point phase space density correlation is not an artifact of assumptions made in the analysis. The assumptions lead to the specific form of divergence, i.e., logarithmic divergence, as presented above. In order to elaborate the point, here we discuss another derivation of sharp increase of the correlation at small scales. Note that the derivation presented here does not involve triplet closure or solving differential moment equation as presented in the paper. Rather, it is based on small scale singularity of two point evolution in collisionless limit. By taking the limit $1 \to 2$ of two point evolution equation of phasestrophy, the mixing term (the left hand side) is zero up to collisions. By retaining small but finite collisions, we have $T(1,2) \to -\langle \delta f(1) C(\delta f(2)) \rangle \cong \nu \langle \delta f(1) \delta f(2) \rangle$. Since $P(1,2)$ is finite in this limit, we have steady solution for phasestrophy as $\langle \delta f(1) \delta f(2) \rangle \sim \nu^{-1} P$. Thus at small scales, the correlation becomes large for small ν. Physically, the sharp correlation indicates formation of singular structures at small scales. In broader context, examples of such structure include caviton in Langmuir turbulence,[41] clumps in resistive drift wave turbulence,[42] granulations in 1D plasmas,[16] etc. In this model, singular structures are trapped ion granulations, clusters of resonating trapped ions.

III. SPECTRUM BALANCE EQUATION AND ITS IMPLICATION

So far, we have discussed the dynamics of trapped ion granulations in phase space and derived the correlation for incoherent fluctuation at steady state. Here, we discuss its macroscopic implication by integrating over energy and by deriving the spectrum balance equation (Eq. (36)). Integrating Eq. (30) over energy gives

$$\left\langle \frac{\widetilde{\delta n_i}(1)}{n_0} \frac{\widetilde{\delta n_i}(2)}{n_0} \right\rangle \cong 64\pi^2 \epsilon_0 v_{thi}^6 \int_{-\bar{E}_<}^{\bar{E}_>} (\tau_{cl}(x_-, y_-, E_-) - \tau_c) d\bar{E}_- \int_0^\infty d\bar{E}_+ \bar{E}_+ P(\bar{E}_+)$$
$$= \frac{8\pi\sqrt{\epsilon_0} v_{thi}^3 \sqrt{6}}{\sqrt{e}|v_{Di}|k_0} \left(\sqrt{1-l^2} - |l| \cos^{-1}|l| \right) \sum_{\mathbf{k}} \frac{2\mathrm{Im}\chi_i \mathrm{Im}\chi_e}{|\partial\chi/\partial\omega_{\mathbf{k}}||\mathrm{Im}\chi|} \sqrt{\bar{E}_{\mathbf{k}}^{res}} \left\langle \frac{\widetilde{\delta n_i}}{n_0} \widetilde{\delta f}_i(\bar{E}_{\mathbf{k}}^{res}) \right\rangle_{\mathbf{k}}. \quad (31)$$

Here, the lefthand side is the correlation of granulation charge density. In the righthand side, we assumed that the small scale correlation from the relative coordinate is dominated by the correlation life time. The energy integral was performed with the cut-off determined from $\tau_{cl}(x_-, y_-, E_{>,<}) - \tau_c \to 0$ and $l^2 \equiv e(k_0^2 x_-^2 + k_0^2 y_-^2/3)$. It is useful to write the balance relation in Fourier components. This can be achieved by Fourier transforming in $\mathbf{x}_-$ and by integrating over k_x spectrum,[43] to yield the spectrum balance equation

$$\left\langle \frac{\widetilde{\delta n_i}(1)}{n_0} \frac{\widetilde{\delta n_i}(2)}{n_0} \right\rangle_{k_y} = 8\pi\sqrt{\epsilon_0} v_{thi}^3 \frac{F(k_y)}{|v_{Di}|k_0} \sum_{\mathbf{k}} \frac{\mathrm{Im}\chi_i \mathrm{Im}\chi_e}{|\partial\chi/\partial\omega_{\mathbf{k}}||\mathrm{Im}\chi|}$$
$$\times \sqrt{\bar{E}_{\mathbf{k}}^{res}} \langle \frac{\widetilde{\delta n_i}}{n_0} \widetilde{\delta f}_i(\bar{E}_{\mathbf{k}}^{res}) \rangle_{\mathbf{k}}. \quad (32)$$

$F(k_y)$ is the spatial form factor of the spectrum emitted by granulations and is given by

$$F(k_y) = \frac{2\sqrt{6}}{\sqrt{e}} \int \frac{dk_x}{k_0} \left(\frac{k_0}{2\pi} \right)^2 \int dx_- dy_- e^{-i\mathbf{k}\cdot\mathbf{x}_-} (\sqrt{1-l^2} - |l| \cos^{-1}|l|). \quad (33)$$

The integration can be performed[43] to give

$$F(k_y) = \sqrt{2} \frac{k_0^2}{k_y^2} \left(1 - J_0 \left(\frac{\sqrt{3} k_y}{\sqrt{e} k_0} \right) \right). \quad (34)$$

Details of the calculation for $F(k_y)$ are given in the Appendix. Finally, by noting that the charge density correlation spectrum can be approximated[22] as

$$\left\langle \frac{\widetilde{\delta n_i}(1)}{n_0} \frac{\widetilde{\delta n_i}(2)}{n_0} \right\rangle_{k_y} \cong 8\pi\sqrt{\epsilon_0} v_{thi}^3 \sqrt{\bar{E}_{k_y}^{res}} \left\langle \frac{\widetilde{\delta n_i}}{n_0} \widetilde{\delta f}_i \left(\bar{E}_{k_y}^{res} \right) \right\rangle_{k_y}, \quad (35)$$

we have the spectrum balance equation for $\langle \widetilde{\delta n_i} \widetilde{\delta f}_i \rangle_{k_y}$

$$\sqrt{|\bar{E}_{k_y}^{res}|} \left\langle \frac{\widetilde{\delta n_i}}{n_0} \widetilde{\delta f}_i \left(\bar{E}_{k_y}^{res} \right) \right\rangle_{k_y}$$
$$\cong \frac{F(k_y)}{k_0 |v_{di}|} \int \frac{dk_y'}{k_0} \frac{\mathrm{Im}\chi_i \mathrm{Im}\chi_e}{|\partial\epsilon/\partial\omega_k||\mathrm{Im}\chi|} \sqrt{|\bar{E}_{k_y'}^{res}|} \left\langle \frac{\widetilde{\delta n_i}}{n_0} \widetilde{\delta f}_i \left(\bar{E}_{k_y'}^{res} \right) \right\rangle_{k_y'}. \quad (36)$$

Here, $\bar{E}_{\mathbf{k}}^{res}$ is assumed to be independent of k_x, which is typically true for $k_x^2 \rho^2 \ll 1$. Within the same accuracy, the k_x sum in the production term was performed. We note that a similar equation was derived for collisionless trapped *electron* turbulence with granulations.[21] In that equation, free energy is in electrons and dissipation arises from ion Landau damping. Here, the balance equation is extended to collisionless trapped *ion* turbulence with granulations. Free energy is in ions and dissipation arises from electron collisions. We also note that Eq. (36) is homogeneous equation in the spectrum amplitude. This is since energy integral is performed

This article is copyrighted as indicated in the article. Reuse of AIP content is subject to the terms at: http://scitation.aip.org/termsconditions. Downloaded to IP: 35.8.11.3 On: Tue, 26 Jan 2016 19:00:16

over the extent $\Delta E \sim \tau_c^{-1}/(k_0 v_{Di})$ and amplitude dependence cancels. Then, Eq. (36) may be solved to obtain "eigenvalue condition," which schematically is

$$|\mathrm{Im}\chi| \sim \frac{F|\mathrm{Im}\chi_i \mathrm{Im}\chi_e|}{k_0|v_{di}||\partial\chi/\partial\omega_k|}. \tag{37}$$

Equation (37) describes "fluctuation-dissipation" type balance at steady state with trapped ion granulations (Fig. 7). Ion free energy $\propto \mathrm{Im}\chi_i$ is released via dynamical friction on electrons $\propto \mathrm{Im}\chi_e$. The process exerts a drag on trapped ion granulations in plasmas, leading to Cerenkov emission of wake fields attached to granulations. Differently put, we may say granulations are dressed by wakes. This is analogous to wakes of water waves caused by ships moving through the water.[44] The emitted spectrum in turn absorbed in plasmas $\propto |\mathrm{Im}\chi|$. The balance between the two leads to steady state.

A consequence from the spectrum balance equation is that granulations can broaden the frequency spectrum. Physically put, trapped ion granulations emit waves, whose frequency need not satisfy dispersion relation $\omega \neq \omega_{\mathbf{k}}$. Then, fluctuation spectrum can contain those supported not by eigenmodes and hence broadens. The frequency broadening is evaluated as follows. Within the framework presented in the paper, the potential fluctuation is supported via emission from granulations $e\widetilde{\phi}_{\mathbf{k}\omega}/T_e = \chi(\mathbf{k},\omega)^{-1}\int d^3 v \widetilde{\delta f}_{i,\mathbf{k}\omega}$. Then, the spectrum intensity $I_{\mathbf{k}\omega} \sim \langle \hat{\phi}^2 \rangle_{\mathbf{k}\omega}$ is

$$I_{\mathbf{k}\omega} \sim \frac{\int \sqrt{E}_1 dE_1 \sqrt{E}_1 dE_2 \langle \widetilde{\delta f}_i(1)\widetilde{\delta f}_i(2)\rangle_{\mathbf{k}\omega}}{|\chi(\mathbf{k},\omega)|^2} \sim \frac{\int \sqrt{E}_1 dE_1 \sqrt{E}_1 dE_2 \langle \widetilde{\delta f}_i(1)\widetilde{\delta f}_i(2)\rangle_{\mathbf{k}} 2\pi\delta\left(\omega_{\mathbf{k}} - \omega_{Di}\bar{E}_+\right)}{\left(\partial\chi/\partial\omega_{\mathbf{k}}\right)^2(\omega-\omega_{\mathbf{k}})^2 + |\mathrm{Im}\chi|^2}. \tag{38}$$

Then, the line width of the frequency spectrum is $\Delta\omega \equiv |\mathrm{Im}\chi|/|\partial\chi/\partial\omega_{\mathbf{k}}|$. The line width caused by the emission from granulations is then

$$\Delta\omega \sim \frac{F|\mathrm{Im}\chi_i||\mathrm{Im}\chi_e|}{k_0|v_{di}||\partial\chi/\partial\omega_k|^2}. \tag{39}$$

Thus, $\Delta\omega$ scales as ion free energy ($\propto \mathrm{Im}\chi_i$) and electron dissipation ($\propto \mathrm{Im}\chi_e$). This is plausible since dynamics of trapped ion granulations are controlled by dynamical friction on electrons. Importantly, this result indicates that to recover non-trivial physics of trapped ion granulations, non-adiabatic electrons are essential. The feature may be checked by numerical or/and physical experiments. Quantitatively, using representative plasma parameters $\epsilon_0 \sim 1/3$, $\tau \sim 1$, $\eta_i \sim \eta_e \sim 1$, $\omega_{\mathbf{k}}/\nu_{e,eff} \sim 0.8$, we find $\Delta\omega/\omega_{\mathbf{k}} \sim 0.16$. Thus, granulations can appreciably contribute to frequency broadening. As a caveat, we note that the analysis presented here emphasizes the effect of trapped ion granulations and requires modes to be oversaturated to achieve stationary state. Hence, $\Delta\omega$ is simply due to emission from granulations. However, in reality, mode-mode coupling of unstable modes, etc., can contribute to broaden in addition to trapped ion granulations. Calculation of $\Delta\omega$ with mode-mode coupling will require the inclusion of unstable spectrum of waves, which will be pursued in future.

IV. CONCLUSION AND DISCUSSION

In this paper, we have discussed dynamics of trapped ion granulations and its macroscopic implications. Testable predictions are summarized in Table I. More specifically, we have discussed that.

(1) Microscopic dynamics of trapped ion granulations are formulated in terms of two point phase space density correlation, or phasestrophy. Phasestrophy is produced through the release of free energy by electron dynamical friction exerted on trapped ion granulations (Eq. (26)). Phasestrophy is torn apart by random $E \times B$ scattering and relative toroidal precession of the two points (Eq. (20)).
(2) Stationary phasestrophy was derived (Eq. (30)). As two points in phase space approaches, phasestrophy increases logarithmically. The sharp correlation is contrasted to the correlation predicted from quasilinear calculation. Deviation of phasestrophy from the quasilinear prediction can be thought of as an indication of the presence of trapped ion granulations in turbulence.
(3) A spectrum balance equation (Eq. (36)) was derived and was solved to obtain the "fluctuation-dissipation" balance relation (Eq. (37)). At macroscopic level, stationary state can be achieved when trapped ion granulations, dragged by electrons, emit waves and waves are in turn absorbed in plasmas (Fig. 7).
(4) The frequency line width was predicted (Eq. (39)). The line width depends on ion free energy and electron dissipation. Thus, non-adiabatic electrons are essential to have non-trivial dynamics of trapped ion granulations. Quantitatively, we find that $\Delta\omega/\omega_{\mathbf{k}} \sim 0.16$ and hence granulations can contribute to frequency broadening appreciably.

As a caveat, we note that the analysis presented here assumes oversaturated modes, in order to elucidate physical

TABLE I. A summary of relevant feature of trapped ion granulations.

	Predictions	Relevant feature
Characteristic scales	$\Delta x \sim \Delta y \lesssim k_0^{-1} \sim \Delta_c$ $\Delta E \lesssim T_i/(\omega_{di}\tau_c)$	Spatially smaller than Δ_c need resolve broadened resonance in energy
Phasestrophy	$\langle \widetilde{\delta f}_i(1)\widetilde{\delta f}_i(2)\rangle \cong (\tau_{cl}(x_-,y_-,E_-) - \tau_c)P(1,2)$	Logarithmic increase in correlation at small scales $\lim_{1\to 2}\langle \widetilde{\delta f}_i \widetilde{\delta f}_i\rangle \gg \tau_c D_\perp \langle f\rangle'^2$
Line width	$\Delta\omega \sim \frac{F\mathrm{Im}\chi_i\mathrm{Im}\chi_e}{k_0\lvert v_{di}\rvert\lvert\partial\chi/\partial\omega_k\rvert^2}$	$\propto \lvert\mathrm{Im}\chi_i\rvert\lvert\mathrm{Im}\chi_e\rvert$ $\rightarrow$ determined by ion free energy *and* electron dissipation

This article is copyrighted as indicated in the article. Reuse of AIP content is subject to the terms at: http://scitation.aip.org/termsconditions. Downloaded to IP: 35.8.11.3 On: Tue, 26 Jan 2016 19:00:16

contribution from trapped ion granulations. However, in reality, trapped ion granulations can be immersed in the bath of unstable trapped ion modes, which can cause large level of transport with Bohm scaling.[20,24,30] In this case, trapped ion granulations and unstable modes can be coupled together. Formulation of the coupled dynamics will require simultaneous solution of both phasestrophy evolution equation and wave kinetic equation for unstable modes. We also note that the analysis presented here neglects coupling to flows. Flow coupling can enter the granulation dynamics through dynamical friction[25–27] $\propto \mathrm{Im}\chi_{pol}$, absorption via flow resonance,[27] shear enhanced dispersion[28,45] $\tau_{cl}^{-1} \propto (k_\perp^2 D_\perp v_y'^2)^{1/3}$, conversion of poloidal and toroidal flow,[46] etc. Systematic studies on coupled dynamics among granulations, unstable trapped ion modes, and flows, and its implication for transport scaling, etc., will be addressed in future.

ACKNOWLEDGMENTS

We thank Professor X. Garbet, Dr. G. Dif-Pradalier, Dr. Ö. D. Gürcan, Dr. Z. Guo, Professor T. S. Hahm, Professor K. Ida, Professor A. Fujisawa, Professor S. Inagaki, and the participants in the Festival de Theorie for stimulating discussions. This work was supported in part by Grants-in-Aid for Scientific Research of JSPF of Japan (21224014, 23244113, and 25887041), the collaboration programs of the RIAM of Kyushu University and of NIFS (NIFS10KOAP023), Asada Science Foundation, Kyushu University Interdisciplinary Programs in Education and Projects in Research Development, the WCI project 2009-001 of MEST of Korea, the U.S. DoE No. DE-FG02-04ER54738, and the U.S. NSF Grant No. PHY11-25915(KITP).

APPENDIX A: LINEAR THEORY

As a preliminary to nonlinear analysis, we summarize linear feature predicted by the model. From the linear response of trapped ions, $\delta n_{i,\mathbf{k},\omega}^{tr}/n_0 = \chi_{i,\mathbf{k},\omega}^{tr}(e\tilde{\phi}/T_e)$, where χ_i^{tr} is the ion susceptibility, we have

$$\chi_i = \sqrt{2\epsilon_0}\frac{2}{\sqrt{\pi}}P\int \sqrt{\bar{E}}d\bar{E}e^{-\bar{E}}\frac{\omega_{*e}}{\omega-\omega_{Di}\bar{E}}\left(1+\eta_i\left(\bar{E}-\frac{3}{2}\right)\right) - i\sqrt{2\epsilon_0}2\sqrt{\pi}\left|\frac{\omega}{\omega_{Di}}\right|^{3/2}e^{-|\omega/\omega_{Di}|}\frac{\omega_{*e}}{|\omega|}\left(1+\eta_i\left(\left|\frac{\omega}{\omega_{Di}}\right|-\frac{3}{2}\right)\right). \tag{A1}$$

The principal part can be calculated by expanding in powers of ω_{Di}/Ω, where $\Omega = \omega - (5/2)\omega_{Di}$. Here, $(5/2)\omega_{Di}$ is subtracted to increase the convergence of the expansion.[23] Then, the energy integral yields

$$\mathrm{Re}\chi_i^{tr} = \frac{\sqrt{2\epsilon_0}\omega_{*e}}{\Omega}\left(1+\frac{\omega_{Di}}{\Omega}\left(\frac{3}{2}\eta_i-1\right)\right). \tag{A2}$$

The second term in the ion susceptibility, $\mathrm{Im}\chi_i^{tr}$, is due to trapped ion precession resonance. Electron response is

$$\chi_e = 1 - i\sqrt{2\epsilon_0}\frac{2}{\sqrt{\pi}}\frac{\omega_{*e}}{\nu_e^{eff}}(2+3\eta_e). \tag{A3}$$

$\mathrm{Im}\chi_e^{tr}$ is due to dissipative electrons and yields a phase shift in the electron density response. Substituting the results for the quasi-neutrality condition, we have the total susceptibility

$$\chi = 1+\tau+\rho^2k_\perp^2 - \frac{\sqrt{2\epsilon_0}\omega_{*e}}{\Omega}\left(1+\frac{\omega_{Di}}{\Omega}\left(\frac{3}{2}\eta_i-1\right)\right) + i\mathrm{Im}\chi_e - i\mathrm{Im}\chi_i. \tag{A4}$$

Here, $\tau = T_e/T_i$. $\mathrm{Re}\chi = 0$ gives the dispersion relation for trapped ion modes

$$\omega_{\mathbf{k}} = \frac{5}{2}\omega_{Di} + \frac{\sqrt{2\epsilon_0}\omega_{*e}}{2\left(1+\tau+\rho^2k_\perp^2\right)}, \tag{A5}$$

$$\gamma_{\mathbf{k}}^{reactive} = \frac{\sqrt{6\tau}(2\epsilon_0)^{1/4}}{2\left(1+\tau+\rho^2k_\perp^2\right)^{1/2}}\sqrt{\omega_{*i}\omega_{Di}}\sqrt{\eta_i-\eta_{cr}}, \tag{A6}$$

where

$$\eta_{cr} \equiv \frac{2}{3} + \frac{\tau\sqrt{2\epsilon_0}\omega_{*i}}{6\left(1+\tau+\rho^2k_\perp^2\right)\omega_{Di}}. \tag{A7}$$

Depending on parameter regimes, the nature of trapped ion modes is different. Relevant features of linear trapped ion modes are summarized as follows:

(1) Dissipative trapped ion modes (DTIM). This is the well-known trapped ion modes, as discussed by Kadomtsev-Pogutse.[20] The mode propagates in the electron direction, $\omega_{\mathbf{k}} \propto \sqrt{2\epsilon_0}\omega_{*e}$. The mode is destabilized due to electron collision, which causes the phase shift in the electron response. The mode is similar to dissipative trapped electron mode, while DTIM is supported by trapped ions and has larger wave length. The latter follows from the fact that DTIM must satisfy $\omega_{bi} > \omega_k$, which leads to $k_\theta\rho_i < \epsilon_0/q$.

(2) Fluid-like collisionless trapped ion modes (CTIM). In the collisionless limit, trapped ion modes have two distinct branches. The first one is fluid like instability, which occurs for $\eta_i \gg \eta_{cr}$. Note that the mode is unstable when $\omega_{*i}\omega_{Di} \propto \nabla p_i \cdot \nabla B > 0$ and so is analogous to interchange like instability. In this respect, the fluid like CTIM is analogous to toroidal ion temperature gradient (ITG). The difference is that the mode has longer wave length and is supported by trapped ions.

(3) CTIM driven by resonance. When CTIM is close to marginal or driven weakly, i.e., $\eta_i \gtrsim \eta_{cr}$, the mode has different characters. In this case, $\omega_{\mathbf{k}} \propto \omega_{Di}$, so the mode propagates in the ion direction. Thus, the resonance with precessing trapped ions becomes important. In this case, the growth rate is given by

$$\gamma_{lin}^{res} = \frac{|\mathrm{Im}\chi_i| - |\mathrm{Im}\chi_e|}{|\partial\chi/\partial\omega_{\mathbf{k}}|}. \tag{A8}$$

Here, the absolute value is inserted to clarify the sign dependence.

This article is copyrighted as indicated in the article. Reuse of AIP content is subject to the terms at: http://scitation.aip.org/termsconditions. Downloaded to IP: 35.8.11.3 On: Tue, 26 Jan 2016 19:00:16

APPENDIX B: DERIVATION OF $F(k_y)$

Here, we perform integral in $F(k_y)$. Transforming the spatial variables via

$$\varrho^2 = e\left(k_0^2 x_-^2 + k_0^2 y_-^2/3\right); \quad x_- = \frac{1}{k_0\sqrt{e}}\varrho\cos\vartheta;$$
$$y_- = \frac{\sqrt{3}}{k_0\sqrt{e}}\varrho\sin\vartheta, \tag{B1}$$

we have

$$F(k_y) = \frac{2\sqrt{6}}{\sqrt{e}}\int\frac{dk_x}{k_0}\frac{1}{(2\pi)^2}\frac{\sqrt{3}}{e}\int_0^1\varrho d\varrho\left(\sqrt{1-\varrho^2}-\varrho\cos^{-1}\varrho\right)$$
$$\times\int_0^{2\pi}d\vartheta\exp\left(-i\frac{k_x}{\sqrt{e}k_0}\varrho\cos\vartheta\right)\exp\left(-i\frac{\sqrt{3}k_y}{\sqrt{e}k_0}\varrho\sin\vartheta\right). \tag{B2}$$

The integral can be performed by noting that

$$\exp\left(-i\frac{k_x}{\sqrt{e}k_0}\varrho\cos\vartheta\right) = \sum_m e^{im\vartheta}(-i)^m J_m\left(\frac{k_x}{\sqrt{e}k_0}\varrho\right), \tag{B3}$$

$$\exp\left(-i\frac{\sqrt{3}k_y}{\sqrt{e}k_0}\varrho\sin\vartheta\right) = \sum_m e^{im\vartheta}(-1)^m J_m\left(\frac{\sqrt{3}k_y}{\sqrt{e}k_0}\varrho\right), \tag{B4}$$

and by using the Neumann's addition theorem for Bessel functions

$$J_0(\beta\varrho) = \sum_m (i)^m J_{-m}\left(\frac{\sqrt{3}k_y}{\sqrt{e}k_0}\varrho\right)J_m\left(\frac{k_x}{\sqrt{e}k_0}\varrho\right), \tag{B5}$$

where $\beta^2 = k_x^2/(ek_0^2) + (3k_y^2)/(ek_0^2)$. Then, we finally have

$$F(k_y) = \frac{2\sqrt{6}}{\sqrt{e}}\int\frac{dk_x}{k_0}\frac{1}{2\pi}\frac{\sqrt{3}}{e}\int_0^1\varrho d\varrho J_0(\beta\varrho)\left(\sqrt{1-\varrho^2}-\varrho\cos^{-1}\varrho\right)$$
$$= \sqrt{2}\frac{k_0^2}{k_y^2}\left(1-J_0\left(\frac{\sqrt{3}k_y}{\sqrt{e}k_0}\right)\right). \tag{B6}$$

[1]I. B. Bernstein, J. M. Greene, and M. D. Kruskal, Phys. Rev. **108**, 546 (1957).
[2]D. Lynden-Bell, Mon. Not. R. Astron. Soc. **136**, 101 (1967).
[3]T. H. Dupree, Phys. Fluids **25**, 277 (1982).
[4]P. W. Terry, P. H. Diamond, and T. S. Hahm, Phys. Fluids B **2**, 2048 (1990).
[5]Y. Kosuga and P. H. Diamond, Phys. Plasmas **19**, 072307 (2012).
[6]N. Carlevaro, D. Fanelli, X. Garbet, P. Ghendrih, G. Montani, and M. Pettini, Plasma Phys. Controlled Fusion **56**, 035013 (2014).
[7]H. L. Berk, B. N. Breizman, and N. V. Petviashvili, Phys. Lett. A **234**, 213 (1997).
[8]H. L. Berk, B. N. Breizman, J. Candy, M. Pekker, and N. V. Petviashvili, Phys. Plasmas **6**, 3102 (1999).
[9]M. Lesur, Y. Idomura, and X. Garbet, Phys. Plasmas **16**, 092305 (2009).
[10]M. K. Lilley, B. N. Breizman, and S. E. Sharapov, Phys. Plasmas **17**, 092305 (2010).
[11]R. M. Nyqvist, M. K. Lilley, and B. N. Breizman, Nucl. Fusion **52**, 094020 (2012).
[12]M. K. Lilley and R. M. Nyqvist, Phys. Rev. Lett. **112**, 155002 (2014).
[13]M. J. Hole and M. Fitzgerald, Plasma Phys. Controlled Fusion **56**, 053001 (2014).
[14]B. B. Kadomtsev and O. P. Pogutse, Phys. Rev. Lett. **25**, 1155 (1970).
[15]T. H. Dupree, Phys. Rev. Lett. **25**, 789 (1970).
[16]T. H. Dupree, Phys. Fluids **15**, 334 (1972).
[17]T. H. Dupree, Phys. Fluids **21**, 783 (1978).
[18]M. Lesur and P. H. Diamond, Phys. Rev. E **87**, 031101(R) (2013).
[19]M. Lesur, P. H. Diamond, and Y. Kosuga, Plasma Phys. Controlled Fusion **56**, 075005 (2014).
[20]B. B. Kadomtsev and O. P. Pogutse, Nucl. Fusion **11**, 67 (1971).
[21]P. H. Diamond, P. L. Similon, P. W. Terry, C. W. Horton, S. M. Mahajan, J. D. Meiss, M. N. Rosenbluth, K. Swartz, T. Tajima, and R. D. Hazeltine, in *Plasma Physics and Controlled Nuclear Fusion Research 1982* (IAEA, Vienna, 1983), Vol. 1, p. 259.
[22]H. Biglari, P. H. Diamond, and P. W. Terry, Phys. Fluids **31**, 2644 (1988).
[23]W. M. Tang, J. C. Adam, and D. W. Ross, Phys. Fluids **20**, 430 (1977).
[24]T. S. Hahm and W. M. Tang, Phys. Plasmas **3**, 242 (1996).
[25]Y. Kosuga, P. H. Diamond, L. Wang, Ö. D. Gürcan, and T. S. Hahm, Nucl. Fusion **53**, 043008 (2013).
[26]Y. Kosuga and P. H. Diamond, Plasma Fusion Res. **5**, S2051 (2010).
[27]Y. Kosuga and P. H. Diamond, Phys. Plasmas **18**, 122305 (2011).
[28]Y. Kosuga, S. I. Itoh, P. H. Diamond, K. Itoh, and M. Lesur, Plasma Fusion Res. **9**, 3403018 (2014).
[29]G. Depret, X. Garbet, P. Bertrand, and A. Ghizzo, Plasma Phys. Controlled Fusion **42**, 949 (2000).
[30]A. Ghizzo, D. D. Sarto, X. Garbet, and Y. Sarazin, Phys. Plasmas **17**, 092501 (2010).
[31]G. Darmet, P. Ghendrih, Y. Sarazin, X. Garbet, and V. Grandgirard, Commun. Nonlinear Sci. Numer. Simul. **13**, 53 (2008).
[32]P. H. Diamond, S.-I. Itoh, and K. Itoh, *Modern Plasma Physics Volume1: Physical Kinetics of Turbulent Plasmas* (Cambridge University Press, Cambridge, 2011).
[33]L. Wang and T. Hahm, Phys. Plasmas **16**, 062309 (2009).
[34]S. T. Tsai and L. Chen, Phys. Fluids B **5**, 3284 (1993).
[35]L. Chen, Phys. Plasmas **1**, 1519 (1994).
[36]F. Zonca and L. Chen, Phys. Plasmas **3**, 323 (1996).
[37]T. Boutros-Ghali and T. H. Dupree, Phys. Fluids **24**, 1839 (1981).
[38]B. H. Hui and T. H. Dupree, Phys. Fluids **18**, 235 (1975).
[39]T. H. Dupree, C. E. Wagner, and W. M. Manheimer, Phys. Fluids **18**, 1167 (1975).
[40]R. H. Berman, D. J. Tetreault, and T. H. Dupree, Phys. Fluids **26**, 2437 (1983).
[41]V. Zakharov, Sov. Phys. JETP **35**, 908 (1972).
[42]P. Terry and P. Diamond, Phys. Fluids **28**, 1419 (1985).
[43]G. S. Lee and P. H. Diamond, Phys. Fluids **29**, 3291 (1986).
[44]J. Lighthill, *Waves in Fluids* (Cambridge University Press, Cambridge, 1978).
[45]H. Bilari, P. H. Diamond, and P. W. Terry, Phys. Fluids B **2**, 1 (1990).
[46]Y. Kosuga, S. I. Itoh, P. H. Diamond, and K. Itoh, Plasma Phys. Controlled Fusion **55**, 125001 (2013).

This article is copyrighted as indicated in the article. Reuse of AIP content is subject to the terms at: http://scitation.aip.org/termsconditions. Downloaded to IP: 35.8.11.3 On: Tue, 26 Jan 2016 19:00:16